

Self-consistent thermal-opto-electronic model for the dynamics in high-power semiconductor lasers

Uwe Bandelow¹, Mindaugas Radziunas¹, Hans Wenzel²

submitted: February 27, 2025

¹ Weierstrass Institute

Mohrenstraße 39

10117 Berlin

Germany

E-Mail: uwe.bandelow@wias-berlin.de

mindaugas.radziunas@wias-berlin.de

² Ferdinand-Braun-Institut

Leibniz Institut für Höchstfrequenztechnik

Gustav-Kirchhoff-Straße 4

12489 Berlin

Germany

E-Mail: hans.wenzel@fbh-berlin.de

No. 3179

Berlin 2025



Edited by
Weierstraß-Institut für Angewandte Analysis und Stochastik (WIAS)
Leibniz-Institut im Forschungsverbund Berlin e. V.
Mohrenstraße 39
10117 Berlin
Germany

Fax: +49 30 20372-303
E-Mail: preprint@wias-berlin.de
World Wide Web: <http://www.wias-berlin.de/>

Self-consistent thermal-opto-electronic model for the dynamics in high-power semiconductor lasers

Uwe Bandelow, Mindaugas Radziunas, Hans Wenzel

Abstract

High-power broad-area diode lasers (BALs) generate significant heat, impacting performance. A 2+1 dimensional traveling wave (TW) model incorporates heating effects through an iterative coupling of electro-optical (EO) and heat-transport (HT) solvers. This method analyzes heat sources, temperature profiles, and thermally induced refractive index changes.

Broad-area lasers (BALs) are crucial for high-performance laser systems and material processing due to their small size and efficiency, producing tens of watts from single devices. However, they exhibit chaotic spatio-temporal dynamics above threshold. High-power lasers generate significant heat, raising the internal temperature and impacting operation. A key effect is the formation of a thermal lens, where the refractive index increases in the hot center, causing slight focusing near the facet. While thermal lenses are well-studied in continuous wave (CW) lasers, they are usually neglected in pulsed operation due to longer thermal build-up times. However, the small heated region near the active layer has a much shorter build-up time, leading to dynamic thermal lensing. We show, that short-term local heating can affect optical pulse formation.

Earlier models, though detailed, overlooked device design and needed a lot of computing power. We propose a physically realistic and yet numerically applicable thermal model, coupled to a dynamical electro-optical (EO) model for the optical field and carrier dynamics along the quantum-well active zone of the laser. A numerical tool, BALaser, is used for accurately simulating these effects. It allows for design optimizations and has been applied to beam shaping, stabilization, and external feedback. Here, the focus is on two topics: filamentation and the effects of temperature changes.

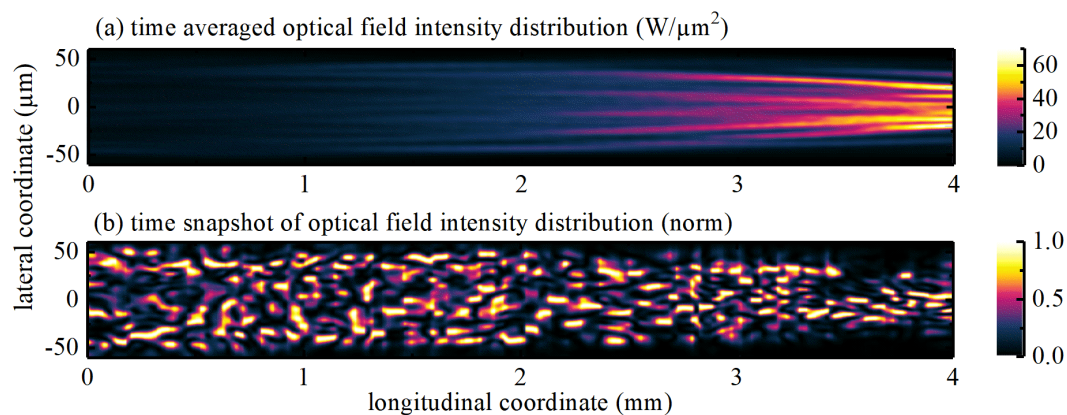


Figure 1: Top view on the optical intensity distribution in the active region of a BA laser under continuous wave (CW) high power operation, calculated with the model of section 1. (a) time averaged, (b) time snapshot of intensities laterally normalized at each longitudinal position [1].

1 The electro-optical (EO) model

Our mathematical model is a hybrid combination of a traveling-wave (TW) model in the (x, z) plane shown in Fig.1, a model of current flow and a thermal model, both in 3D domain, parametrized by the

variable z . The slowly varying complex amplitudes $u^\pm(x, z, t)$ of the optical field obey a TW equation coupled to a diffusion equation for the carrier density $N(x, z, t)$ [1]

$$\frac{1}{v_g} \partial_t u^\pm = \left[\frac{-i}{2k} \partial_{xx} \mp \partial_z + \frac{G - \alpha}{2} + i\delta - \mathcal{D} \right] u^\pm + F_{sp}^\pm \quad (1)$$

$$\frac{\partial N}{\partial t} = \frac{\partial}{\partial x} \left(D_{\text{eff}}(N) \frac{\partial N}{\partial x} \right) + \frac{j(x, z, t)}{ed} - R(N, u^\pm, \mathcal{D}), \quad (2)$$

$$\mathcal{D} u^\pm = \frac{g_r}{2} (u^\pm - p^\pm), \quad \frac{\partial p^\pm}{\partial t} = \gamma (u^\pm - p^\pm) + i\delta \omega p^\pm. \quad (3)$$

The optical gain G depends on N and the operator \mathcal{D} models its dispersion in terms of a Lorentzian [2] with amplitude g_r . The amplitudes u^\pm are coupled to each other by reflecting boundary conditions at the facets. The detuning $\delta(N, T)$ accounts for built-in index changes, carrier density and temperature dependent index changes, as well as for the Kerr effect. The optical loss α includes internal background absorption, the free carrier absorption and the two-photon absorption in the active region [3]. The numerical integration of the TW-model equations are performed using parallel computing and distributed memory paradigm at the WIAS in Berlin. Typical 1 ns-transient simulations of 4 mm-long and 100 μm -broad laser using 20-30 parallel processes can be made in 5-10 minutes. Details on the efficiency of the code are given in [4].

Current spreading and current self-distribution in the p-doped layers play an important role in BA lasers [5, 6, 7]. They largely influence the Joule heating - one of the heat sources, which is proportional to the square of the current density,

$$\mathbf{j} = \sigma \nabla \varphi_p \quad (4)$$

with the electrical conductivity σ . The quasi-Fermi potential φ_p of the holes obeys a Laplace equation $\nabla(\sigma \nabla \varphi_p) = 0$ in the p-doped region [8, 6], which completes our EO model.

2 The thermal model

The thermal model bases on the classical macroscopic *heat-flow equation*,

$$c_h \frac{\partial T}{\partial t} - \nabla [\kappa_L \nabla T] = h(N, \mathbf{j}, \|u\|^2), \quad (5)$$

with the heat capacity c_h , the heat conductivity κ_L , and the heat sources h , which depend on the carrier density, current density, and field intensity distributions in the laser, which result from the EO model. The heat sink temperature T_{HS} enters via a boundary condition into the model. Reversely, the temperature T acts back on the wave propagation mainly via the detuning δ by the thermally induced refractive index, and implicitly influences the gain, distribution functions, and the diffusion as well as recombination terms in Eq. (2).

The *heat sources* h of the model include the Joule heat, that is essentially generated in the p-doped region, the heat source due to absorption of stimulated emitted photons, the recombination heat in the active region, and the quantum defect heat generated in the active region as a result of incomplete energy transfer from the carrier reservoir to the radiation field. They are explicitly given in [1] and are derived from corresponding expressions given in [9, 3, 10]. Furthermore, in this paper we neglect Thompson-Peltier heat [9, 3] as the overall impact is expected to be small[11]. The heat sources

obtained with the dynamic EO-solver exhibit strong variations on short time scales, which however have only a marginal impact on the temperature distribution.

It is unreasonable to solve the heat-flow equation (5) over tens of microseconds with the sub-ps temporal resolution of the opto-electronic model in the large spatial domain of the whole device. An estimation [1] showed, that the generated heat during a 1 ns simulation interval is spread around the active region by only about 100 nm. Heat flow is therefore negligible when simulating short transients and the thermally induced index can be calculated via an ordinary differential equation which is integrated much easier in each node of the spatial grid.

The extremely long thermal build up in the case of CW operation cannot be calculated with this approximation. But in the later quasi-steady state, the rate of heat generation can be decomposed in a time-constant mean contribution \bar{h} and a contribution $h_{\text{fluct}} = h - \bar{h}$ fluctuating around zero. Accordingly, the heat-flow equation (5) is split into

$$0 = \nabla \kappa_L \nabla \bar{T} + \bar{h} \quad \text{and} \quad (6)$$

$$c_h \frac{\partial T_{\text{fluct}}}{\partial t} = \nabla \kappa_L \nabla T_{\text{fluct}} + h_{\text{fluct}}. \quad (7)$$

For the numerical solution we apply an iterative approach [1]. In the first step of the iteration the EO model is solved under isothermal conditions with $T = T_{\text{HS}}$. During this run, we set $\bar{h} = 0$. In all following iterations, \bar{h} is taken as the temporal average of the total heat production of the last part of the iteration before. The iterations are repeated until the temperature and near-field intensity distributions of consecutive iteration steps are sufficiently close to each other. A detailed description of the numerical implementation is given in Ref. [12].

3 Results

The static HT-problem, with time-averaged heat sources, is solved iteratively together with the EO solver. Under short pulse operation the thermally induced index distribution can be obtained by neglecting the heat flow. Although the temperature increase is small, a waveguide is introduced here within a few-ns-long pulse, resulting in significant near field narrowing. We further show that a beam propagating in a waveguide structure utilized for BA lasers does not undergo filamentation due to spatial holeburning. This remains a high-dimensional spatio-temporal phenomenon, that can not fully be explained by simplified models, such as the focusing nonlinear Schrödinger equation. Moreover, our results indicate that in BALs a clear mode structure is visible which is neither destroyed by the chaotic dynamics nor by longitudinal effects.

References

- [1] U. Bandelow, M. Radziunas, A. Zeghuzi, H.-J. Wünsche, and H. Wenzel, "Dynamics in high-power diode lasers," *Proc. SPIE 11356, Semiconductor Lasers and Laser Dynamics IX 11356*(113560W), pp. 1–14, 2020.
- [2] C. Z. Ning, R. A. Indik, and J. V. Moloney, "Effective Bloch equations for semiconductor lasers and amplifiers," *IEEE J. Quantum Electron.* **33**(9), pp. 1543–1550, 1997.
- [3] H. Wenzel and A. Zeghuzi, "High-Power Lasers," in *Handbook of Optoelectronic Device Modeling & Simulation*, J. Piprek., ed., ch. 33, pp. 15–58, CRC Press, Taylor & Francis Group, 1 ed., 2017.

- [4] M. Radziunas, "Modeling and simulations of broad-area edge-emitting semiconductor devices," *The Intl. Journ. of High Performance Computing Applications* **4**(32), pp. 512–522, 2018.
- [5] A. Zeghuzi, M. Radziunas, H.-J. Wünsche, J.-P. Koester, H. Wenzel, U. Bandelow, and A. Knigge, "Traveling wave analysis of non-thermal far-field blooming in high-power broad-area lasers," *IEEE J. Quantum Electron.* **55**(2), p. 2000207, 2019.
- [6] M. Radziunas, A. Zeghuzi, J. Fuhrmann, T. Koprucki, H. J. Wünsche, H. Wenzel, and U. Bandelow, "Efficient coupling of the inhomogeneous current spreading model to the dynamic electro-optical solver for broad-area edge-emitting semiconductor devices," *Opt. Quantum Electron.* **49**(10), pp. 1–8, 2017.
- [7] W. B. Joyce, "Role of the conductivity of the confining layers in DH-laser spatial hole burning effects," *IEEE J. Quantum Electron.* **18**(12), pp. 2005–2009, 1982.
- [8] G. R. Hadley, J. P. Hohimer, and A. Owyong, "Comprehensive modeling of diode arrays and broad-area devices with applications to lateral index tailoring," *IEEE J. Quantum Electron.* **24**(11), pp. 2138–2152, 1988.
- [9] U. Bandelow, H. Gajewski, and R. Hünlich, "Fabry-Pérot laser: Thermodynamics - based modeling of edge - emitting quantum well lasers," in *Optoelectronic Devices - Advanced Simulation and Analysis*, J. Piprek, ed., ch. 3, pp. 63–85, Springer, New York, 2005.
- [10] G. K. Wachutka, "Rigorous thermodynamic treatment of heat generation and conduction in semiconductor device modeling," *IEEE Trans. Comput. Des.* **9**(11), pp. 1141–1149, 1990.
- [11] A. Zeghuzi, H.-J. Wünsche, H. Wenzel, M. Radziunas, J. Fuhrmann, A. Klehr, U. Bandelow, and A. Knigge, "Time-dependent simulation of thermal lensing in high-power broad-area semiconductor lasers," *IEEE J. Sel. Top. Quantum Electron.* **25**(6), p. 1502310, 2019.
- [12] M. Radziunas, J. Fuhrmann, A. Zeghuzi, H. J. Wünsche, T. Koprucki, C. Brée, H. Wenzel, and U. Bandelow, "Efficient coupling of dynamic electro-optical and heat-transport models for high-power broad-area semiconductor lasers," *Opt. Quantum Electron.* **51**(69), 2019.